Fast adaptative interferometer on dynamic reflection hologram in CdTe:V

Salvatore Di Girolamo, Alexei A. Kamshilin, Roman V. Romashko, Yuri N. Kulchin, Jean-Claude Launay

Fast adaptive interferometer on dynamic reflection hologram in CdTe:V

Salvatore Di Girolamo and Alexei A. Kamshilin

Physics Dept., University of Kuopio, P.O. Box 1627, FIN-70211, Kuopio, Finland
alexei.kamchiline@uku.fi

Roman V. Romashko and Yuriy N. Kulchin

Optoelectronics Lab., Institute of Automation & Control Processes, FEB RAS, 5 Radio str. Vladivostok, 690041 Russia
romashko@delphin.marine.su

Jean Claude Launay

Institute of Condensed Matter and Chemistry of Bordeaux- ICMCB/CNRS, University Bordeaux 1, 87 Avenue Dr A. Schweitzer, 33608 Pessac Cedex, France
launay@icmcb-bordeaux.cnrs.fr

Abstract: We present an adaptive interferometer based on the reflection dynamic hologram recorded in photorefractive CdTe:V crystal with no external electric field. Linear phase-to-intensity transformation is achieved by vectorial mixing of two waves with different polarization states (linear and elliptical) in the anisotropic diffraction geometry. Comparison of reflection and transmission geometries considering both sensitivity and adaptability is carried out. It is shown that the reflection geometry is characterized by better combination of these parameters provided that the crystal possesses high enough concentration of photorefractive centers.

OCIS codes: 190.7070 Two-wave mixing; 120.5050 phase measurements

References and links

1. S. I. Stepanov, "Application of photorefractive crystals," Rep. Prog. Phys. **57**, 39-116 (1994).
2. I. M. Rossomakhin and S. I. Stepanov, "Linear adaptive interferometers via diffusion recording in cubic photorefractive crystals," Opt. Commun. **86**, 199-204 (1991).
3. R. K. Ing and J.-P. Monchalin, "Broadband optical detection of ultrasound by two-wave mixing in a photorefractive crystal," Appl. Phys. Lett. **59**, 3233-3235 (1991).
4. P. Delaye, A. Blouin, D. Drolet, L.-A. de Montmorillon, G. Roosen, and J.-P. Monchalin, "Detection of ultrasonic motion of a scattering surface using photorefractive InP:Fe under an applied dc field," J. Opt. Soc. Am. B **14**, 1723-1734 (1997).
5. A. Blouin and J.-P. Monchalin, "Detection of ultrasonic motion of a scattering surface by two-wave mixing in a photorefractive GaAs crystal," Appl. Phys. Lett. **65**, 932-934 (1994).
6. B. Campagne, A. Blouin, L. Pujol, and J.-P. Monchalin, "Compact and fast response ultrasonic detection device based on two-wave mixing in a gallium arsenide photorefractive crystal," Rev. Sci. Instrum. **72**, 2478-2482 (2001).
7. A. A. Kamshilin and A. I. Grachev, "Adaptive interferometer based on wave mixing in a photorefractive crystal under alternating electric field," Appl. Phys. Lett. **81**, 2923-2925 (2002).
8. M. P. Petrov, S. I. Stepanov, and A. V. Khomenko, *Photorefractive crystals in coherent optical systems* (Springer-Verlag, Berlin, Germany 1991).
9. B. I. Sturman, E. V. Podivilov, K. H. Ringhofer, E. Shamonina, V. P. Kamenov, E. Nippolainen, V. V. Prokofiev, and A. A. Kamshilin, "Theory of photorefractive vectorial wave coupling in cubic crystals," Phys. Rev. E **60**, 3332-3352 (1999).
10. A. A. Kamshilin, E. Raita, and A. I. Grachev, "Polarization degree of freedom in photorefractive two-wave coupling," in *Trends in Optics and Photonics: Photorefractive Effects, Materials, and Devices*, P. Delaye, C. Denz, L. Mager, and G. Montemezzani, eds., **87**, 476-482 (2003).
11. R. V. Romashko, Y. N. Kulchin, and A. A. Kamshilin, "Linear phase demodulation via reflection photorefractive holograms," in *Trends in Optics and Photonics (TOPS): Photorefractive Effects, Materials,*

#76862 - $15.00 USD Received 7 November 2006; accepted 20 December 2006

and Devices, G. Zhang, D. Kip, D. D. Nolte, and J. Xu, eds., Vol. **99** of OSA Proceedings Series (Optical Society of America, Washington, D.C., 2005), pp. 675-680.
12. L.-A. de Montmorillon, P. Delaye, J.-C. Launay, and G. Roosen, "Novel theoretical aspects on photorefractive ultrasonic detection and implementation of a sensor with an optimum sensitivity," J. Appl. Phys. **82**, 5913-5922 (1997).
13. J. W. Wagner and J. B. Spicer, "Theoretical noise-limited sensitivity of classical interferometry," J. Opt. Soc. Am. B **4**, 1316-1326 (1987).
14. K. Paivasaari, H. Tuovinen, A. A. Kamshilin, and E. Raita, "Highly sensitive photorefractive interferometry using external ac-field," in *Trends in Optics and Photonics (TOPS): Photorefractive Effects, Materials, and Devices*, G. Zhang, D. Kip, D. D. Nolte, and J. Xu, eds., Vol. **99** of OSA Proceedings Series (Optical Society of America, Washington, D.C., 2005), pp.681-686.

1. Introduction

An adaptive interferometer using two-wave mixing in photorefractive crystal (PRC) has simple and highly sensitive technique for measurement phase variations under unstable environmental conditions [1]. Two key parameters of any adaptive interferometer are sensitivity to small phase excursions and response time, which defines how fast the device is capable to adapt with variable environment. It is very often required in industrial applications to achieve high rejection rate of vibrations at 50/60 Hz. Consequently, the response time of photorefractive crystal should be faster than 300 μs which corresponds to the low-frequency cut-off of 500 Hz. Among known photorefractive crystals only highly photoconductive semi-insulators (InP, GaAs, CdTe) possess such fast response time. However, light-beam coupling in these crystals is smaller than in ferroelectrics such as $BaTiO_3$ or $LiNbO_3$. Therefore, it has to be enhanced by applying strong dc or ac electric field to the crystal. In many practical applications it is desirable to rid off using strong electric field. It is well known that dynamic hologram can be recorded in any PRC owing to diffusion of charge carriers (without external field). However the efficiency of diffusion-type hologram is not high enough. Moreover, such hologram cannot be directly used for efficient phase demodulation since it is characterized by inherent phase shift 0 (or π) between interfering beams resulting in the least efficient phase-to-intensity transformation.

Several modifications of the diffusion-mode TWM interferometer have been proposed [2-6]. Rossomakhin & Stepanov installed a quarter-wave plate and properly oriented polarizer behind the crystal operating in the regime of anisotropic diffraction to fulfill the quadrature condition of linear phase demodulation [2]. Later on, Ing & Monchalin described linear phase demodulator in PRC oriented for isotropic diffraction in which mixed light beams pass through a phase retarder first and then are split by a polarizing beamsplitter into two photodiodes detecting the light power in the differential mode [3]. Blouin & Monchalin combined both previous approaches by using anisotropic diffraction and differential light-power detection after the polarizing beam-splitter [5]. Note that in all the described above cases the linear regime of phase demodulation is achieved either by installation of polarizer or polarization beam-splitter before the photo-detector, which introduces optical losses leading to worsening of sensitivity. Alternative modification was recently proposed in Ref. [7] where it was shown that coupling of two waves with different polarization states in the geometry of anisotropic diffraction results in $\pm\pi/2$-phase shift between transmitted and diffracted waves thus providing optimal conditions for linear phase demodulation. In contrast to previous proposals no polarizing element is to be installed behind the crystal and the entire light power of mixed beams is received by a single photo-detector. This type of light beam coupling in PRC is referred to as vectorial wave mixing (VWM) [7]. In this paper we extend the vectorial-wave-mixing approach to the geometry of counter-propagating beams in which the reflection-type dynamic holograms are recorded. Sensitivity and adaptability of VWM-interferometer were compared for reflection and transmission geometries of dynamic holograms recorded in different CdTe crystals without external electric field. We show that the reflection geometry is characterized by better combination of sensitivity and adaptability providing that the crystal has high enough concentration of photorefractive centers.

#76862 - $15.00 USD Received 7 November 2006; accepted 20 December 2006

2. Vectorial wave mixing in reflection and transmission geometry

It is known that space-charge field created without applying external electric field to PR-crystal is spatially shifted from the intensity distribution by a quarter of the interference-pattern period [8]. In other words there is a phase shift of $\pi/2$ between these two distributions. In the framework of conventional scalar approach which treats photorefractive hologram as periodic refractive-index pattern which either spatially coincides or is in counter phase with the intensity distribution of interference pattern. By adding the $\pi/2$ phase shift that accompanies reflection from the index grating, we obtain phase difference between transmitted signal wave and diffracted reference wave being equal to 0 or π. Therefore, conventional two-wave coupling via hologram recorded in the diffusion mode does not support linear transformation of small transient phase modulation into intensity modulation. However, if light diffraction has anisotropic character (i.e. diffraction is accompanied by change of the polarization state), the linear phase-to-intensity transformation can be achieved even in the diffusion recording mode when linearly and elliptically polarized waves are mixed [7]. It occurs because the inherent $\pi/2$-phase difference between orthogonal components (*x* and *y*) of elliptically polarized wave is transferred into an interference term of the transmitted signal and diffracted reference waves [7].

To observe efficient anisotropic diffraction from the reflection hologram, the grating vector should be oriented along one of the principal crystallographic axes of the crystal as it is shown in Fig 1(a). Note that this condition is different for the transmission geometry where anisotropic diffraction is the most pronounced if the interfering beams propagate at small angle in respect to the $[\bar{1}10]$-axis while the grating vector is parallel to the [110]-axis [9], as it is shown in Fig. 1(b). For CdTe crystal, which belongs to the symmetry group $\bar{4}3m$, the coupled wave equations for light beams interacting via dynamic hologram recorded in the diffusion regime can be written as

$$\begin{cases} \left(\dfrac{\partial}{\partial z}+\dfrac{\alpha}{2}\right)\vec{A}_R = \kappa\hat{H}\vec{A}_S \\ \left(g\dfrac{\partial}{\partial z}+\dfrac{\alpha}{2}\right)\vec{A}_S = -\kappa\hat{H}\vec{A}_R \end{cases}. \tag{1}$$

Here $\vec{A}_{S,R}$ are two-dimensional vectors describing both amplitude and polarization state of the object and reference wave, respectively; α is the light absorption coefficient, and g is the recording geometry factor, which is equal to +1 in the case of transmission geometry and -1 for the reflection geometry. The dimensionless 2×2 matrix $\hat{H}$ depends on the relative orientation of the grating vector, crystallographic axes, and the polarization components of the light field [9]. This matrix defines the character of light diffraction from the dynamic holographic grating: isotropic or anisotropic. The coupling constant κ for the hologram recorded in the diffusion mode can be represented as [8]

$$\kappa = -\frac{\sqrt{2R}}{1+R}\frac{\pi n_0^3 r_{41}}{\lambda}\frac{E_D}{1+E_D/E_q} \text{ with } E_D = \frac{2\pi}{\Lambda}\frac{k_B T}{e} \text{ and } E_q = \frac{e\cdot N_A}{\varepsilon\varepsilon_0}\frac{\Lambda}{2\pi}, \tag{2}$$

where n_0 is the refractive index; r_{41} is electro-optical coefficient; E_D is the diffusion electric field; E_q is the saturation field; e is the electron's charge; N_A is the concentration of the photorefractive centers; Λ is the spatial period of dynamic hologram; R is the intensity ratio of the reference to the object beam in the input of the crystal; k_B is the Boltzman's constant; and T is the temperature; $\varepsilon\varepsilon_0$ is a dielectric constant. As we show below, the sensitivity of an adaptive interferometer is primarily defined by the coupling constant, κ: The larger κ; the higher sensitivity to small phase changes can be achieved. Therefore, one could expect an increase of the sensitivity while switching from the transmission to the reflection geometry because of the significant diminishing of the grating period, Λ. However, this increase of κ

#76862 - $15.00 USD Received 7 November 2006; accepted 20 December 2006

depends on the concentration of the photorefractive centers, N_A. Note that the coupling constant in the reflection geometry may become even smaller than that in the transmission geometry if the concentration of the photorefractive centers is small ($N_A < 2\times10^{16}$ cm^{-3} for CdTe with $n_0 = 2.85$) due to reduction of the saturation field E_q.

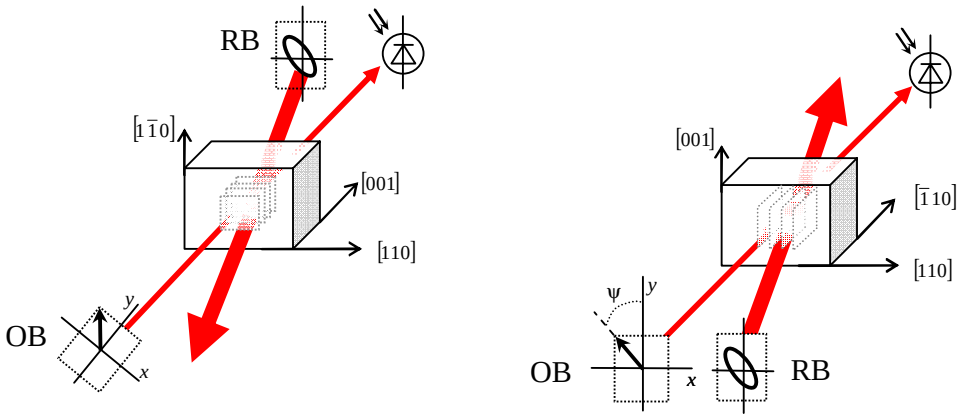

a *b*

Fig. 1. Adaptive interferometer based on diffusion hologram recorded in photorefractive crystal in reflection (*a*) and transmission (*b*) geometry; RB and OB are reference and object beams respectively.

For the light beam interaction depicted in Fig. 1, the matrix $\hat{H}$ is the same for both transmission and reflection geometries: $\hat{H} = \begin{pmatrix} 0 & 1 \\ 1 & 0 \end{pmatrix}$ indicating that pure anisotropic diffraction occurs when *x*-polarized component of the input beam diffracts into *y*-polarized component and vice versa. Our aim is to calculate the change of object beam power at the output of the crystal when small transient phase shift φ is introduced into one of the interacting beams. A simple analytical solution of Eq. (1) can be found [10] for the transmission geometry of Fig. 1(b) if we consider interaction of linearly and circularly polarized beams assuming that the intensity modulation of the interference pattern, $m = 2\sqrt{R}/(R+1)$ is small and invariable inside the crystal. In this case the light power, P_S, of the object beam transmitted through crystal of thickness L is:

$$P_S = P_0 \exp(-\alpha L)\left[\cos^2(\kappa L) + R\sin^2(\kappa L) - \sqrt{\frac{R}{2}}\sin(2\kappa L)\sin(2\psi - \varphi)\right]. \qquad (3)$$

Here P_0 is the power of the object beam entered into the crystal and ψ is the angle between the polarization plane of the linearly polarized object wave and the crystallographic axis [001]. Equation (3) shows that the small transient phase shift is linearly transferred into the light power modulation at either $\psi = 0$ or $\psi = \pi/2$. Note that in case of equal polarization states (either linear or elliptical) of reference and object beams the variation of the output-beam light power is always proportional to $\cos(\varphi)$, what makes interferometer least sensitive to small transient change of phase. We were not yet able to solve the system of Eq. (1) for the reflection geometry (g = -1) analytically. However its numerical solution reveals the same principal features as for the transmission geometry [11]: (i) linear phase-to-intensity transformation when the linearly polarized wave is mixed with the circularly polarized wave and (ii) achievement of the highest transformation rate at $\psi = 0$ or $\pi/2$.

#76862 - $15.00 USD Received 7 November 2006; accepted 20 December 2006

3. Sensitivity of an adaptive interferometer

3.1. Theoretical estimation

The common way of estimating performance of an adaptive interferometer is to compare its sensitivity with that of classical homodyne interferometer free of optical losses [4,12]. It is well known that the classical interferometer adjusted to the quadrature condition allows measurements of the smallest phase change. Therefore the ratio of the minimal detectable phase change measured by an adaptive interferometer (when signal is equal to noise, *SNR* = 1) and the classical homodyne detection limit characterizes interferometer's sensitivity. It is usually done in conditions when the inevitable shot noise of photo-detector is much larger than all other noises of the measuring system (noise of laser, electronics etc.). Under these conditions, the signal-to-noise ratio can be expressed as [13]:

$$SNR = \frac{\Delta P_S}{Q\sqrt{P_S}} \text{ with } Q = \sqrt{\frac{4\,\Delta f\ h\nu}{\eta}}\ , \tag{4}$$

where P_S is the power of non-modulated object beam received by the photo-detector; ΔP_S is the variation of object beam power caused by phase modulation; η is the quantum efficiency of the photo-detector; $h\nu$ is the photon's energy; and Δf is the frequency bandwidth of the detection electronics. In the classical lossless interferometer under the quadrature conditions one can find that $P_S = 2P_0'$ and $\Delta P_S \approx 2P_0'\varphi$ for small phase variations ($\varphi << 1$), where P_0' is the power of object beam and it is equal to that of reference beam. The classical homodyne detection limit, $\varphi_C^{\lim}$, can be now found from Eq. (4) by equalizing *SNR* to the unity:

$$\varphi_C^{\lim} = \frac{Q}{\sqrt{2P_0'}} = \sqrt{\frac{2\Delta f\ h\nu}{\eta P_0'}}\ . \tag{5}$$

The minimal detectable phase change, $\varphi_A^{\lim}$, of adaptive interferometer operating in the diffusion regime and in the transmission geometry can be found similarly using Eq. (3):

$$\varphi_A^{\lim} = Q\exp\left(\frac{\alpha L}{2}\right)\frac{\sqrt{2}\sqrt{\cos^2(\kappa L) + R\sin^2(\kappa L)}}{\sin(2\kappa L)\cdot\sqrt{RP_0}} \tag{6}$$

Here we neglect all losses of optical elements with the exception of optical absorption of the photorefractive crystal which is essential for the formation of dynamic hologram. P_0 in Eq. (6) is the light power of the object beam in the input of the interferometer. A comparison of adaptive and classical interferometers can be done assuming that the input power of the object beam is the same for both interferometers, $P_0 = P_0'$. Moreover, the wavelength, quantum efficiency of the photo-detector, and the frequency bandwidth are also the same. Therefore the relative detection limit, δ_{rel}, does not depend on the object power and other parameters of the receiver:

$$\delta_{rel} = \frac{\varphi_A^{\lim}}{\varphi_C^{\lim}} = \exp\left(\frac{\alpha L}{2}\right)\sqrt{\frac{1}{2R\sin^2(\kappa L)} + \frac{1}{2\cos^2(\kappa L)}} \tag{7}$$

One can see that δ_{rel} is always larger than the unity, it is infinitely large when $\kappa = 0$, and it decreases with the increase of coupling constant, κ, which indicates improvement of the adaptive interferometer sensitivity to small phase excursions. After measuring the light absorption and the coupling constant, Eq. (7) allows us to find optimal thickness of the crystal

#76862 - $15.00 USD Received 7 November 2006; accepted 20 December 2006

necessary for achieving maximal sensitivity of the adaptive interferometer. An analysis of Eq. (7) reveals that δ_{rel} always diminishes when the beam-intensity ratio R increases. However, for $R > 20$ any further improvement of the interferometer sensitivity becomes insignificant (less than 5%). The usefulness of parameter δ_{rel} for optimization of an adaptive interferometer was underlined in Ref. [12], where coupling of light waves with same polarization was considered. It was shown that the relative detection limit depends only on the imaginary part of the coupling constant [12]. In contrast, here we show that in the case of coupling of two waves with different polarization state, the relative detection limit is a function of the real part of coupling constant. That thus provides efficient phase demodulation even for hologram recorded in the diffusion mode. It is worth reminding that Eq. (7) is applicable only for the two-wave coupling of linearly and circularly polarized waves through a diffusion-recorded dynamic hologram. However, it represents the main features of any VWM interferometer.

3.2. Experimental measurements of the relative detection limit

For the experimental estimation of relative detection limit we have applied the following procedure. Signal-to-noise ratio of an adaptive interferometer SNR_A can be experimentally estimated by use of Eq. (4) if the photo-detector's current is directly proportional to the optical power. We can represent the relative detection limit using Eq. (5) as following

$$\delta_{rel} = \frac{\varphi_A^{\lim}}{\varphi_C^{\lim}} = \frac{SNR_C}{SNR_A} = \frac{\sqrt{2P_0'P_S}}{\Delta P_S}\varphi . \tag{8}$$

Here P_S is the mean light power received by the photo-detector and P_0' is the power of the input object beam in the classical interferometer. All losses of the object light beam in the way between the input of the interferometer and photo-detector have to be taken into account. Optical losses from passive optical elements can be significantly reduced by applying antireflection coating. The largest optical losses are caused by optical absorption in the photorefractive crystal that allows us to readily recalculate the input power of the adaptive interferometer: $P_S = P_0 e^{-\alpha L}$ Considering the situation where the object beam power in classical interferometer, P_0', is equal to the power of object beam entered into the crystal in adaptive interferometer, P_0, we can obtain expression for the relative detection limit:

$$\delta_{rel} = \sqrt{2}\exp\left(\frac{\alpha L}{2}\right)\frac{P_S}{\Delta P_S}\varphi . \tag{9}$$

Here $\Delta P_S/P_S$ is the depth of the photo-detector current modulation caused by the transient phase shift φ, α is the absorption coefficient of the crystal, and L is the crystal thickness. After measuring all these parameters, the relative detection limit is calculated from Eq. (9).

4. Experimental results

4.1. Experimental setup

The performance of an adaptive interferometer with dynamic holograms recorded in the reflection geometry was studied using experimental setup shown in Fig. 2. A comparison of the interferometer sensitivity in the reflection versus transmission geometry was carried out in the same samples simply by introducing the interacting light beams from different facets in accordance with Fig. 1. A solid-state Nd:YAG laser (λ = 1064 nm, output power 500 mW, coherence length > 100 m) was used as a light source. Photorefractive crystals of CdTe:V were grown in CNRS-Bordeaux Institute of Condensed Matter Chemistry by using modified Bridgman technique. The concentration of Vanadium in all studied crystals was 10^{18} cm^{-3}. However, the ingots were grown under slightly different technological conditions. The dimensions of samples and their absorption are summarized in Table 1.

The characterization of the adaptive interferometer was carried out in conditions close to practical applications: we used speckled object beam emerging from the multimode optical

#76862 - $15.00 USD Received 7 November 2006; accepted 20 December 2006

fiber (NA = 0.22, core diameter = 550 μm, length = 8.7 m). To introduce the phase modulation into the object wave part of the fiber (7.7 m) was reeled onto a calibrated piezoelectric transducer with cylindrical shape. Any voltage applied to the piezoelectric cylinder leads to elongation/compression of the reeled fiber resulting in phase modulation of the output speckled wave. The reference beam with Gaussian intensity distribution was split out from the output laser beam and mixed in the photorefractive crystal with the object beam. The holographic principle of beams combining allows us to match successfully different wave-fronts of the reference and object beams, while adaptive properties of the dynamic hologram result in compensation of undesirable slow phase drifts caused by environmental changes. The output radiation from the fiber was collected by lens into a beam spot of 0.8 mm in diameter on the input face of the crystal. The beam spot must have the same size as the reference beam. The intensity of the reference beam was always larger than that of the object beam with intensity ratio $R \approx 16$. Therefore, the condition of small modulation index m under which Eq. (2) and Eq. (3) were derived was satisfied.

Table 1. Parameters of CdTe:V samples

Sample	$L_{(001)}$, mm	$L_{(110)}$, mm	$L_{(1\bar{1}0)}$, mm	α, cm^{-1}
BR-4Z-05	6.65	7.03	6.02	2.0
BL-07-B1	5.87	7.86	7.40	1.7

In Fig. 2, elliptically polarized reference beam was mixed in CdTe crystal with linearly polarized object beam to achieve linear phase-to-intensity transformation. The polarizer was placed at the fiber output to select an appropriate linear polarization state from almost non-polarized light emerged from the multimode fiber. Half-wave and quarter-wave plates installed in the reference beam allow us to adjust its polarization state aiming to achieve the most efficient wave coupling and the highest SNR.

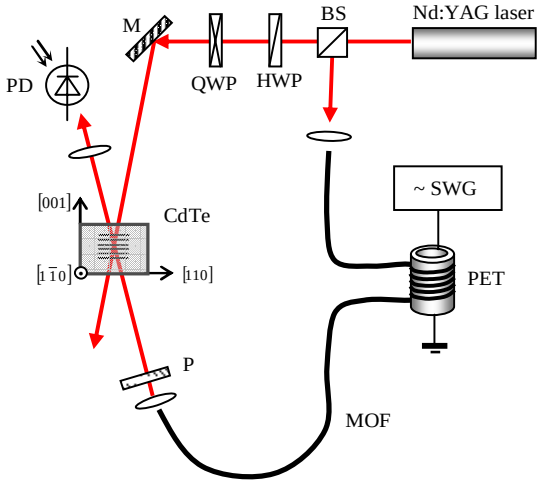

Fig. 2. Schematics of adaptive interferometer based on diffusion dynamic hologram recorded in CdTe crystal: BS is beam splitter; QWP, HWP are quarter- and half-wave plates, respectively; M is a mirror; SWG is a sine wave generator; PET is piezoelectric transducer; MOF is a multimode optical fiber; P is polarizer; PD is photo-detector.

4.2. Sensitivity measurements

Comparison of VWM interferometer sensitivity in different geometries (reflection and transmission) was done by measuring the relative detection limit δ_{rel} as a function of the holographic grating period Λ, which determines the coupling constant in accordance to Eq.

#76862 - $15.00 USD Received 7 November 2006; accepted 20 December 2006

(2). For measurements δ_{rel} we apply sinusoidal voltage to piezo-electric cylinder to introduce into the object beam phase modulation φ with peak-to-peak amplitude of 0.2 radians. This phase modulation results in modulation of photo-detector current at same frequency. The ratio of the peak-to-peak current modulation and its mean level is equal to $\Delta P_S/P_S$. With measured sample absorption α and thickness L, we calculate δ_{rel} from Eq. (9). The dependencies of relative detection limit on spatial period for two CdTe:V crystals are shown in Fig. 3. In transmission geometry the grating period was varied from 5.2 to 0.8 μm by changing the angle between interacting beams from 12 to 89 degrees respectively. However, in the reflection geometry (when grating period reaches its minimum) we were not able to change Λ in significantly wide range, and hence only one experimental point (at Λ = 0.19 μm) corresponding to the reflection hologram is shown in Fig. 3 for both samples.

Figure 3 shows that the slope of the dependence $\delta_{rel}(\Lambda)$ is different for two samples in the transmission geometry (Λ > 0.8 μm). One can see from Eq. (2) and Eq. (7) that only two parameters (r_{41} and N_A) may affect the slope of $\delta_{rel}(\Lambda)$ in the diffusion mode of holographic recording. Since the difference of electro-optic constant r_{41} is hardly possible for crystals of same content, we conclude that the reason for the different slope is different concentration, N_A, of photorefractive centers in these samples: BR-4Z-05 has higher concentration of the centers than BL-07-B1. Note that δ_{rel} decreases in both samples when switching from transmission to reflection geometry. However, the value of δ_{rel} decreasing (or coupling increasing) is much larger for the BR-4Z-05 sample that also relates with higher concentration of the photorefractive centers due to stronger influence of the saturation field on the coupling constant at smaller Λ [see Eq. (2)]. We have observed that δ_{rel} in the reflection geometry slightly depends on the position of hologram recording inside the crystal, which can also be attributed to non-uniform concentration of the photorefractive centers in the samples. It should be noted that δ_{rel} for third CdTe:V sample (having the same concentration of vanadium but grown under slightly different temperature conditions) is comparable with two other samples in the transmission geometry but becomes larger when switching to the reflection geometry. Therefore the concentration of photorefractive centers has to be high enough for efficient beam coupling in the reflection geometry.

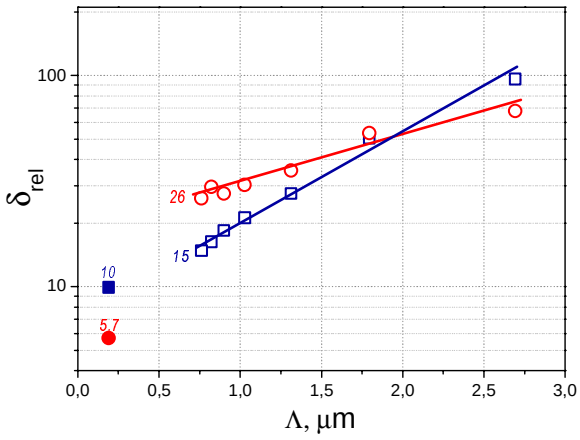

Fig. 3. Relative detection limit of the interferometer as a function of the grating period. Circles relate to the sample BR-4Z-05, squares – to the sample BL-07-B1; open marks correspond to the transmission geometry of hologram recording, while the filled marks – to the reflection geometry.

#76862 - $15.00 USD Received 7 November 2006; accepted 20 December 2006

4.3. Response time of the adaptive interferometer

As known, any adaptive interferometer based on dynamic holograms operates as a high-pass filter [1], as demonstrated in Fig. 4 where we show the dependence of the modulation amplitude of photo-detector's current on the modulation frequency for both samples. These measurements were carried out by applying piezo-ceramic sinusoidal voltage at different frequency with such amplitude as to keep the peak-to-peak phase modulation of the light beam emerged from the multimode fiber at the level of 0.2 radians for any frequency. The intensities of the coupling beams were the same when measured for both samples: I_{REF} = 37.8 W/cm^2 and I_{OBJ} = 2.4 W/cm^2. We define the cut-off frequency, f_{cut}, of our interferometer as the frequency at which the interferometer response drops down to half of the saturation value at high frequencies. The cut-off frequency of the adaptive interferometer is inversely proportional to the response time, τ_R, of the photorefractive crystal [1]: $f_{cut} = (2\pi\tau_R)^{-1}$. One can see that more sensitive sample (BR-4Z-05) has slower response f_{cut} = 180 Hz (τ_R = 0.9 ms) in contrast to less sensitive but faster BL-07-B1 sample: f_{cut} = 750 Hz and τ_R = 0.2 ms.

It is possible to increase the cut-off frequency by increasing the total light intensity I of interacting beams in accordance with well known relation [9]:

$$f_{cut} = \frac{e}{2\pi\varepsilon\varepsilon_0}\frac{\alpha\mu\tau}{h\nu}I\,, \tag{10}$$

where $\mu\tau$ is charge carriers mobility-lifetime product. By reducing the size of both reference and object beams down to 0.6 mm, we increase the intensity to 67.2 W/cm^2 and 3.9 W/cm^2 for the reference and object beams, respectively. In accordance with Eq. (10), we have measured higher cut-off frequency: 300 Hz for BR-4Z-05 sample and to 1250 Hz for BL-07-B1 sample. It is worth noting that cut-off frequency higher than 1 kHz is required for industrial on-line applications, where either object surface is fast moving or efficient noise rejection at frequency 50/60 Hz is desirable.

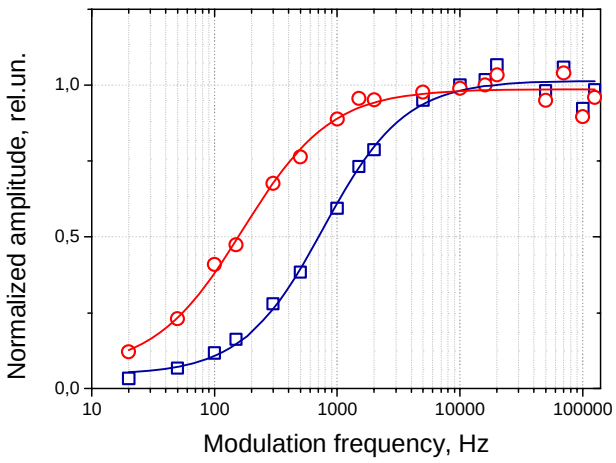

Fig. 4. Frequency response of the adaptive interferometer based on the reflection hologram recorded in CdTe:V crystal. Circles relate to the sample BR-4Z-05, squares – to the sample BL-07-B1.

#76862 - $15.00 USD Received 7 November 2006; accepted 20 December 2006

5. Discussion

Looking at Fig. 3, the sensitivity of VWM interferometer can be essentially improved by switching from transmission to reflection geometry (i.e. by reducing the space period, Λ) if the concentration of photorefractive centers, N_A, is high enough. In the reflection geometry we have got 4.5-fold increase of the sensitivity for BR-4Z-05 sample and 1.5-fold increase for BL-07-B1 sample compared to the best sensitivity obtained in transmission geometry. In the transmission geometry, the diminishing of the spatial period Λ is always accompanied by a decreased overlapping of the reference and object beams (i.e. by decreasing of the interaction length). This is even more pronounced when the diameters of interacting beams are small. Note that the diminishing of the beam diameter leads directly to an increase in the intensity of interacting beams and consequently, to an increase in the cut-off frequency [see Eq. (10)]. Moreover, the minimum L achievable in the transmission geometry is limited by the refraction index of the crystal, which is quite high for CdTe: $n_0 = 2.85$ at $\lambda = 1064$ nm resulting in the minimal Λ of about 0.8 μm. In contrast, in the reflection geometry one can readily achieve a perfect overlapping even for interacting beams of small diameter.

As seen in Fig. 3 the best sensitivity was obtained for the BR-4Z-05 sample in the reflection geometry: the sensitivity of the interferometer using dynamic hologram recorded in photorefractive crystal without any external electrical field and any polarization filtering is only 5.7 times smaller than the sensitivity of classical lossless interferometer. It corresponds to the minimal detectable transient phase excursion of $1.9 \cdot 10^{-9} \mathrm{rad}\sqrt{\mathrm{W/Hz}}$. Such sensitivity is not a record for adaptive interferometers: more sensitive photorefractive beam combiners were reported [4,7,12,14]. However, in all cases either DC [4,12] or AC [7,14] electric field was applied to the crystal. The application of DC electric field requires uniform illumination of the inter-electrodes space or otherwise, the electric field screening leads to diminishing of the beam coupling. Whatever the case, hologram recording under DC-field by light beams of high intensity is hardly possible in fast semiconductors due to crystal overheating and that limits the cut-off frequency. The recording of dynamic hologram under AC-field resolves the field-screening problem but only by application of high-voltage at a frequency much higher than f_{cut} which requires use of expensive power source and generates significant noise. The here proposed technique of vectorial wave mixing via reflection-type dynamic hologram recorded in the diffusion mode is very simple in its implementation and provides good combination of sensitivity and response time. In the reflection geometry interacting beams can be tightly focused in order to increase the light intensity inside the crystal resulting in an increase of the cut-off frequency without significant reduction of the interaction length owing to almost collinear beams propagation. Consequently, high cut-off frequency can be achieved even with relatively low-power laser. In our experiments, diminishing of the beam diameter from 0.8 mm down to 0.6 mm results in two-fold increase of the cut-off frequency, while the interferometer sensitivity was reduced only by ~18% in the reflection geometry (the relative detection limit was increased from 5.7 to 7 for BR-4Z-05 sample, and from 10 to 11.3 for BL-07-B1 sample). This small diminishing of the sensitivity may be explained by not optimal focal length of the lenses used for focusing the interacting beams into the crystal.

6. Conclusion

In this paper we present an adaptive interferometer based on dynamic hologram recorded in semiconductor photorefractive crystal CdTe:V without any external electric field. Linear phase-to-intensity transformation is achieved owing to vectorial mixing of two waves with different polarization states (linear and elliptical) in the geometry of anisotropic diffraction without installing a polarizer after the crystal. Proposed adaptive interferometer has high sensitivity to small transient phase excursions (only 5.7 times worse than the classical homodyne detection limit) and fast response time (0.5 ms) that makes it very prospective for industrial applications.

#76862 - $15.00 USD Received 7 November 2006; accepted 20 December 2006

Acknowledgments

SDG and AAK thank the Academy of Finland for financial support (research project 107554). RVR was funded under the grant MK-1400.2006.2 of the President of Russian Federation. RVR and YNK also acknowledge partial financial support of the Russian Foundation for Basic Research. JCL thanks for financial support of European Space Agency under the ESA contract number 14240/NL/SH.

#76862 - $15.00 USD Received 7 November 2006; accepted 20 December 2006